

Effect of the substrate bias in diamond deposition during hot filament chemical vapor deposition: Approach by non-classical crystallization

Jin-Woo Park¹, Kwang-Ho Kim^{2,3}, Nong-Moon Hwang^{1*,3}

¹Department of Materials Science and Engineering, Seoul National University, 1 Gwanak-ro, Gwanak-gu, Seoul 08826, Korea.

²School of Materials Science and Engineering, Pusan National University, Busan 46241, Korea

³Global Frontier R&D Center for Hybrid Interface Materials, Pusan National University, Busan 46241, Korea

*Corresponding author

DOI: 10.5185/amlett.2018.2082

www.vbripress.com/aml

Abstract

The effect of the substrate bias on the diamond deposition was studied using a hot filament chemical vapor deposition (HFCVD) reactor. Both growth rate of diamonds and sp^3/sp^2 ratio increased with increasing the substrate bias from -200 V to $+45$ V. At $+60$ V where the DC glow discharge occurred, however, the data deviated significantly from the tendency. These results were explained by the new concept of non-classical crystallization, where a building block of diamond growth is a charged nanoparticle rather than an atom. Based on the previously reported experimental confirmation of the gas phase generation of negatively-charged diamond nanoparticles, the bias effect on the diamond deposition behavior could be consistently explained. Copyright © 2018 VBRI Press.

Keywords: Bias, diamond film, nanoparticles, hot filament cvd, microstructure.

Introduction

The film growth mechanism in the chemical vapor deposition (CVD) process has been explained typically by the terrace-ledge-kink (TLK) model, which is based on the belief that the building block of thin films is either an atom or a molecule [1-3]. However, Hwang et al. [4-7] suggested a drastically novel growth mechanism, the theory of charged nanoparticles (TCN), where charged nanoparticles (CNPs) are spontaneously generated in the gas phase and become a building block of thin films or nanostructures. Initially, the TCN was suggested to explain some puzzling phenomena in the diamond CVD process but turned out to be a general growth mechanism of thin films and nanostructures in many CVD and PVD processes [7]. The TCN is unique in explaining successfully the well-known observation of diamond deposition with simultaneous graphite etching without violating the second law of thermodynamics. Besides, it can explain another puzzling observation that diamonds are deposited on the silicon substrate whereas porous skeletal soot is deposited on the iron substrate under the same processing condition in the diamond CVD process [6-8]. In order to explain the evolution of dense crystalline films by a building block of CNPs, CNPs should undergo epitaxial recrystallization upon landing on the growing surface and not leave over any void behind. To follow such a deposition behavior, CNPs should have a liquid-like property. Hwang [7] suggested that the charge weakens the bond strength and as a result

the CNPs could have a liquid-like property. Weakening the bond strength of Si-H and Si-Si by the charge was confirmed using ab-initio calculations in SiH_4 and Si_2H_6 by Clare et al. [9]. For a singly-charged nanoparticle, this effect of weakening the bond strength would decrease with increasing the size of CNPs. Therefore, the smaller CNPs would be more liquid-like than the larger ones. And the smaller CNPs would be favorable for the epitaxial recrystallization under the same substrate temperature.

It was shown that the nanoparticles generated in the gas phase are mostly negatively charged during hot filament CVD (HWCVD) of diamond deposition process [7, 8]. In the case of the DC plasma diamond CVD process, a positively biased substrate produced diamonds, whereas a negatively biased substrate produced an amorphous or graphite phase carbon [10]. Homann et al. [11] examined the difference between positively and negatively charged carbon particles by time-of-flight measurements during their study of the oxy-hydrocarbon flame and suggested that the negatively-charged nanoparticles consist of pure carbon, whereas the positively-charged ones are hydrogenated. Based on these results, Hwang and Kim [12] suggested that negative CNPs have a diamond structure and positive CNPs have an amorphous structure with a hydrogenated surface.

Recently, Park et al. [13] confirmed that the diamond nanoparticles are generated in the gas phase by capturing

them on the membrane of the TEM grid under the typical processing condition of diamond deposition using a HFCVD reactor. Based on the observation that the number density of captured diamond nanoparticles decreases with decreasing the electric bias from positive to negative bias, they suggested that the diamond nanoparticles in the gas phase are negatively charged. Motivated by these previous researches, we try to re-examine the bias effect on the diamond deposition behavior. The purpose of this paper is to study the effect of bias applied to the substrate in a HFCVD reactor. To apply the electric bias to the substrate, the substrate holder was connected with the DC electric bias supply during diamond deposition. In order to compare the growth rate and the sp^3/sp^2 ratio according to the substrate bias, the deposited diamond was observed by field emission scanning electron microscopy (FESEM) and was analyzed by a Raman spectrometer.

Experimental procedure

The HFCVD reactor for diamond deposition is schematically drawn in **Fig. 1**. The filament consisted of three tungsten wires of 0.5 mm ϕ twisted to a 9-turn coil of 8-mm ϕ . The filament and substrate temperatures were 2100 $^{\circ}$ C and 900 $^{\circ}$ C, respectively. The reaction pressure was 20 torr. The flow rates of CH₄ and H₂ were 1 and 99 standard cubic centimeters per minute (sccm), respectively, which was controlled by a mass flow controller. Bare and pretreated Si wafers of 0.7 mm thickness were used as substrates for diamond deposition. The pretreated Si wafers were ultrasonically treated for 10 min with mixtures of ethanol and nano diamond powder of the size of 4-6 nm (PlasmaChem, PL-D-G01). Then they were ultrasonically cleaned for 10 min with ethanol. To apply the DC bias, a square stainless-steel substrate holder (10 \times 10 mm²) was used. The silicon substrate on the holder was 11.3 mm below the hot filament.

The DC electric bias was applied to the substrate holder with respect to the grounded chamber so that the electric field was formed between the stainless-steel substrate holder and the grounded chamber. When the

distance between the filament and the substrate is 11.3 mm, the bias above +50 V and below -250 V tends to generate the DC glow discharge, which is revealed by the abrupt increase of the current in the power supply. Under the biases of -200, -100, 0, and +45 V, the DC glow discharge did not occur during the deposition for 8 h. In addition, to compare the deposition behavior under the DC glow discharge, the deposition was done for 8 h under the bias of +60 V, which generated the DC glow discharge.

The microstructure of deposited diamonds was observed by field emission scanning electron microscopy (FESEM, SU70, Hitachi). The deposited diamonds were analyzed using a Raman spectrometer (LabRam Aramis, Horiba Jobin Yvon) with an Ar-ion laser beam at an exciting radiation wavelength of 514.5 nm and a spot size of 1 μ m.

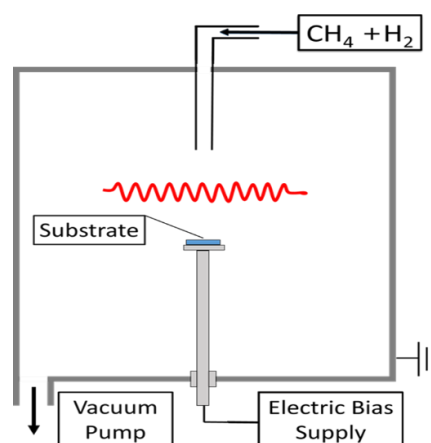


Fig. 1 Schematic of the experimental setup for diamond deposition using the HFCVD reactor. The diamond deposition was done with the bias applied to the stainless-steel substrate holder.

Result

Fig. 2 is the FESEM image showing the diamond particles deposited for 8 h on the bare silicon substrate with the substrate biases of -200, -100, 0, +45 and +60 V at the substrate temperature of 900 $^{\circ}$ C and the hot filament temperature of 2100 $^{\circ}$ C under 20 torr. Since the

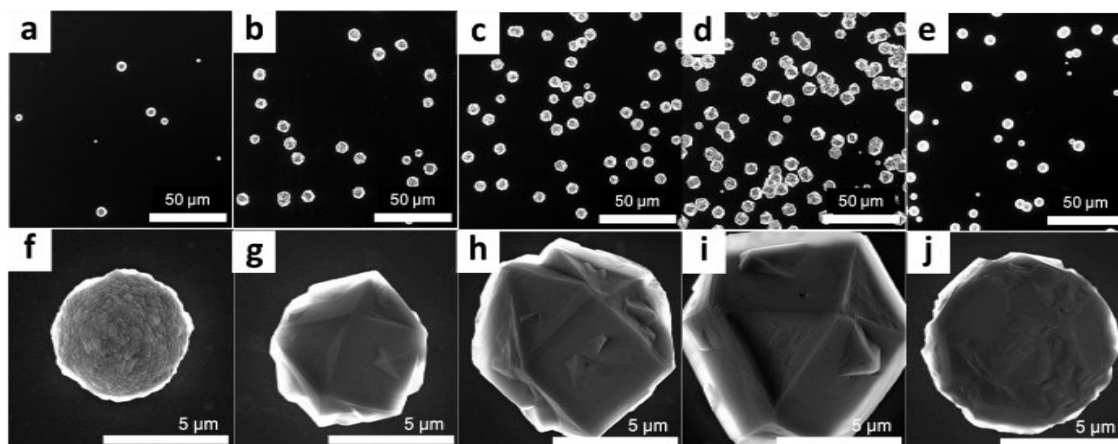


Fig. 2. FESEM images of diamonds deposited for 8 h on the bare silicon substrate with substrate biases of (a) -200, (b) -100, (c) 0, (d) +45 and (e) +60 V and (f) - (j) their magnified images showing each diamond particle of (a) - (e), respectively.

silicon substrate was not pretreated, the entire substrate surface was not covered with the diamond film. The amount of deposited diamonds, which is equivalent to the deposition rate, is represented by the percentage of diamond coverage on the surface. In **Fig. 2(a)-(d)**, it is clear that the diamond coverage increased monotonically with increasing the substrate bias from -200 V to $+45$ V. However, it should be noted that the coverage decreased at the substrate bias of $+60$ V in **Fig. 2(e)** where the DC glow discharge was generated. Quantitatively, the percentages of coverage were 1.7%, 6.2%, 9.7%, 18.2% and 6.3% respectively for -200 , -100 , 0 , $+45$ and $+60$ V, as shown in **Fig. 3**.

Each diamond particle in **Fig. 2(a)-(e)**, which was observed in a higher magnification of FESEM, is shown respectively in **Fig. 2(f)-(j)**. The diamond particles at the substrate biases of -100 , 0 and $+45$ V have the morphology of a cuboctahedron with well-defined facets, as shown in **Fig. 2(g)-(i)**. This is in contrast with **Fig. 2(f)**, where the substrate bias of -200 V was applied, the particle has a spherical shape with numerous nanometer-sized nodules on the surface, which is known as a cauliflower structure. In **Fig. 2(j)**, where the substrate bias of $+60$ V was applied, the particle has an overall spherical shape, which is partially covered with crystalline facets. The size of deposited particles increased slightly with increasing the substrate bias from -200 V to $+45$ V. But at the substrate bias of $+60$ V, the size decreased.

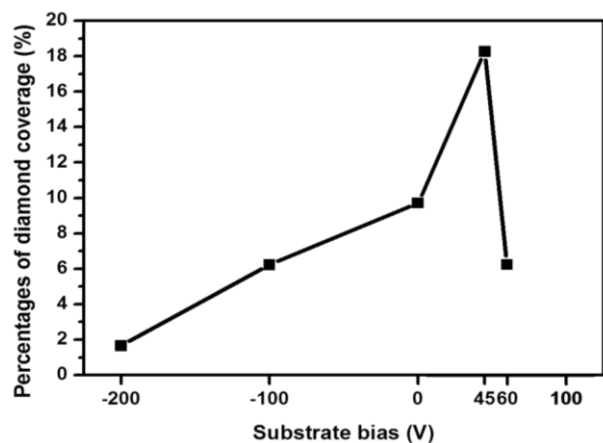


Fig. 3. Percentages of the diamond coverage on the substrate surface at biases of -200 , -100 , 0 , $+45$ and $+60$ V.

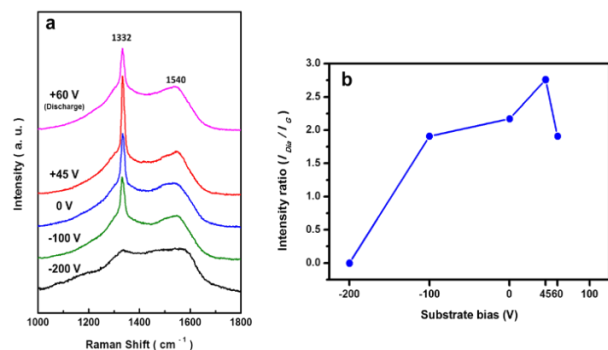


Fig. 4. (a) Raman spectra of deposited particles in **Fig. 2(f)-(j)**. (b) Intensity ratio (I_{Dia}/I_G) of Raman spectra plotted against the substrate bias.

To examine the characteristics of deposited particles shown in **Fig. 2**, the local area of each particle was analyzed by a micro Raman spectrometer with a spot size of $1 \mu\text{m}$. **Fig. 4(a)** shows the Raman spectra of each particle deposited under the substrate biases of -200 V, -100 , 0 , $+45$ and $+60$ V. Raman spectra in **Fig. 4(a)** show a sharp peak at 1332 cm^{-1} , which indicates the diamond [14], for the particle deposited under the biases of -100 , 0 and $+45$ and $+60$ V. However, Raman spectrum of the particle deposited under the substrate bias of -200 V does not show the diamond peak but shows broad D and G bands, which represent the amorphous carbon [14, 15].

It is generally known that the intensity ratio between diamond peak and G-band (I_{Dia}/I_G) increases with increasing the sp^3 content [16-18]. Because of the relationship between the ratio (I_{Dia}/I_G) and the sp^3 content, the intensity ratio of diamond-to-G band was used to determine the sp^3/sp^2 ratio or the diamond content. Therefore, the ratio (I_{Dia}/I_G) can be used to compare the sp^3 content of the particles shown in **Fig. 2**. In **Fig. 4(b)**, the ratio (I_{Dia}/I_G) is plotted as a function of the substrate bias. The ratio increases with increasing the substrate bias, being 0, 1.9, 2.2, and 2.8 respectively for -200 , -100 , 0 , and $+45$ V. At the substrate bias of $+60$ V, however, the ratio is 1.9, which is smaller than that for the bias of $+45$ V. This smaller ratio at the bias of $+60$ V would be attributed to the generation of the DC glow discharge. **Figs. 2-4** show that both diamond coverage and sp^3 content increased with increasing the bias voltage from -200 V to $+45$ V. At the bias of $+60$ V, however, the data did not follow the general trend.

Since the bare silicon substrate was used for deposition in **Fig. 2**, the film was not formed on the entire surface. In order to form a film on the substrate, diamonds were also deposited on the pretreated silicon substrate under the same processing condition as **Fig. 2**. As shown by the FESEM images in **Fig. 5**, the films were formed on the entire surface except **Fig. 5(a)**, where the substrate bias of -200 V was applied. **Fig. 5(b)-(e)** show well-defined facets of diamond films, which is in contrast with the spherical shape and the discontinuous film in **Fig. 5(a)**. Besides, the grain size of diamond films tends to increase with increasing the substrate bias from -100 V to $+45$ V as shown in **Fig. 5(b)-(d)**. The grain size in **Fig. 5(e)** is much smaller than that in **Fig. 5(d)**, which would be also attributed to the generation of the DC glow discharge.

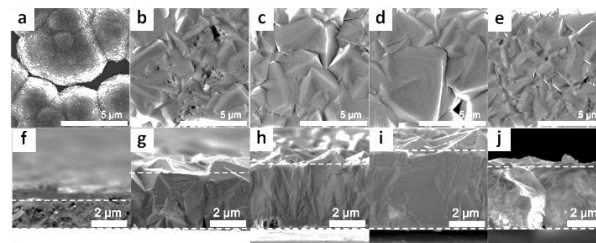


Fig. 5. FESEM images of diamond films deposited for 8 h on the pretreated silicon substrate with substrate biases of (a) -200 , (b) -100 , (c) 0 , (d) $+45$ and (e) $+60$ V and (f) - (j) their cross-sectional images of (a) - (e), respectively.

Fig. 5(f) - (j) show the cross-sectional FESEM images of diamond films of **Fig. 5(a) - (e)**, respectively. The average film thickness, which represents the growth rate, increased with increasing the substrate bias, being 1.5, 3, 3.3, and 4.1 μm respectively for -200 , -100 , 0 and $+45$ V. At $+60$ V, however, the thickness decreased to 3.4 μm . These thickness data are plotted as a function of the substrate bias in **Fig. 6**. This deposition behavior is similar to that on the bare silicon substrate shown in **Fig. 2**.

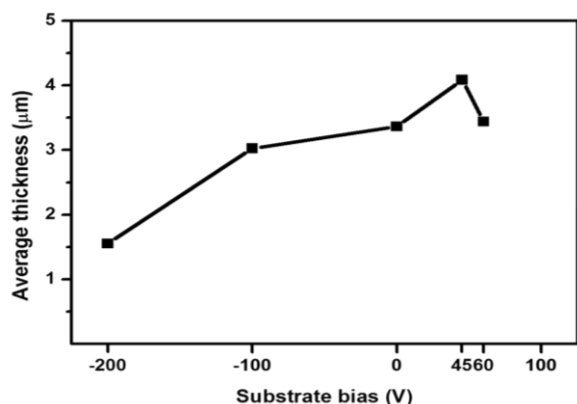


Fig. 6 Average thickness of diamond films deposited under substrate biases of -200 , -100 , 0 , $+45$, and $+60$ V.

As in **Fig. 4**, the films shown in **Fig. 5** were also analyzed by a Raman spectrometer and the intensity ratio ($I_{\text{Dia}}/I_{\text{G}}$) were evaluated as shown in **Fig. 7**. In **Fig. 7(a)**, Raman spectra of the diamond film under the substrate biases of -100 , 0 , $+45$ and $+60$ V reveal a sharp peak for diamond at 1332 cm^{-1} , but those under the substrate bias of -200 V show amorphous carbon with broad D and G bands. Also, the ratio ($I_{\text{Dia}}/I_{\text{G}}$) of diamond films on the pretreated silicon substrate in **Fig. 7(b)** increased with the bias from -200 V to $+45$ V but decreased at the bias of $+60$ V. This deposition behavior has a tendency similar to that of the diamond particles deposited on the bare silicon substrate.

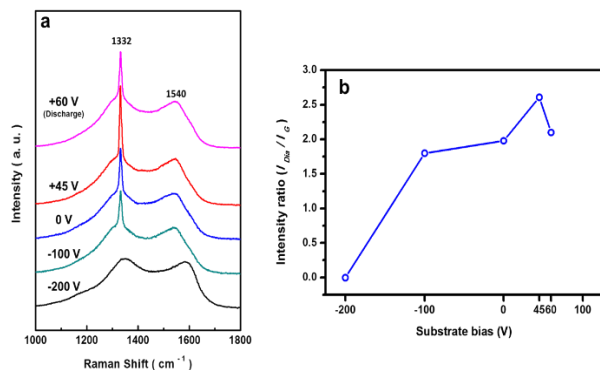


Fig. 7 (a) Raman spectra of deposited films in **Fig. 5(a)-(e)**. (b) Intensity ratio ($I_{\text{Dia}}/I_{\text{G}}$) of Raman spectra plotted against the substrate bias.

Discussion

Figs. 2, 3, 5 and **6** clearly show that the deposition behavior of diamonds is affected by the applied bias.

Previously, such a bias effect was explained by the bombardment of electrons or ions, based on the concept of classical crystallization [19, 20]. However, the non-classical crystallization is now established for the growth of diamond films [7, 8, 21]. In other words, charged diamond nanoparticles are generated in the gas phase and become a building block of diamond films. Recently, Park et al. [13] captured these diamond nanoparticles on the membrane of the TEM grid under a typical processing condition of HFCVD and showed that they are negatively charged.

Therefore, the bias effect in **Figs. 2, 3, 5** and **6** should be approached from the concept of non-classical crystallization. The increase of diamond growth rate with increasing the substrate bias from -200 V to $+45$ V in **Figs. 3** and **6** can be explained by considering that negatively-charged diamond nanoparticles would be repelled from the substrate under the negative bias and attracted toward the substrate under the positive bias. This explanation is valid in the bias range from -200 V to $+45$ V. When the DC glow discharge occurs in the HFCVD reactor by the bias of $+60$ V, the sheath potential builds up on the substrate and would decrease the effect of the positive bias applied to the substrate. This might be related with the lower growth rate of diamonds at $+60$ V than at $+45$ V in **Figs. 3** and **6**.

At $+60$ V, however, not only the growth rate was decreased but also the quality of diamonds was degraded as shown in **Fig. 2(j)**, **Fig. 4(b)** and **Fig. 7(b)**. This degradation of diamond quality would be related with the increase in the size of negatively charged diamond nanoparticles. Under the condition of HFCVD where the DC glow discharge does not occur, negative charges are much more dominant than positive ones, which was revealed in the current measurement using the energy analyzer and the Wien filter by Jeon et al. [22, 23]. This dominance of negative charges would be related with the negative surface ionization of atoms, molecules or clusters on the hot filament. Under this situation, negatively-charged diamond nanoparticles can maintain the small size because the coagulation among them is inhibited due to Coulomb repulsion. When the DC glow discharge occurs, however, not only negative charges but also positive charges are abundantly formed because the plasma provides a bipolar charging condition. Due to the presence of abundant positively-charged species, the size of negatively-charged diamond nanoparticles cannot be maintained small but become larger. On the other hand, Hwang [7] suggested that when the size of charged diamond nanoparticles is increased, the nanoparticles become less liquid-like and their epitaxial recrystallization on the growing diamond surface becomes more difficult, resulting in the degradation of diamond quality. Therefore, the poor quality of diamond at the bias of $+60$ V in **Fig. 2(j)**, **Fig. 4(b)** and **Fig. 7(b)** can be explained by the size increase of the charged diamond nanoparticles in the DC glow discharge.

Then, the increase of the sp^3/sp^2 ratio with increasing the substrate bias from -200 V to $+45$ V in **Figs. 4(b)** and **7(b)** should be explained. Hwang et al. [7, 8, 21]

suggested that the negatively-charged nanoparticles have a diamond phase but the positively-charged nanoparticles are a hydrogenated non-diamond carbon. The positive bias will attract the negatively-charged diamond nanoparticles and repel the positively-charged non-diamond nanoparticles and vice versa for the negative bias. Especially, the Raman spectra of deposited film under the substrate bias of -200 V shown in **Figs. 4(a)** and **7(a)** are dominated by D (~ 1340 cm^{-1}) and G bands (~ 1580 cm^{-1}) and exhibit no diamond peak. It appears that under the bias of -200 V, most of negatively-charged diamond nanoparticles are repelled from the substrate and only positively-charged non-diamond carbon nanoparticles contribute to deposition. This would be why amorphous carbon was deposited under the bias of -200 V.

On the other hand, such a non-diamond carbon phase has a much higher etching rate than the diamond phase. It should be noted that atomically etching takes place under the condition of the gas phase nucleation of carbon in the C-H system [4]. The diamond film would etch much more slowly than the non-diamond carbon film. This high etching rate of the non-diamond carbon phase might be responsible for the low deposition rate under the bias of -200 V as shown in **Figs. 3** and **6**. All the results of the bias effect in this paper would be difficult to explain by the concept of classical crystallization but can be explained consistently within the framework of non-classical crystallization.

Conclusion

According to the deposition behavior of diamonds under the substrate bias during HFCVD, it was shown that the growth rate of diamond and the diamond content increase with increasing the substrate bias. These bias effects could be explained by the concept of non-classical crystallization for diamond growth, where the negatively-charged diamond nanoparticles are generated in the gas phase and become the building block of diamond growth.

Acknowledgements

This work was supported by the Brain Korea (BK21) Program, Republic of Korea, the Asian Office of Aerospace Research and Development (AOARD) (FA2386-15-1-4067), the Global Frontier Program through the Global Frontier Hybrid Interface Materials (GFHIM) (2013M3A6B1078874) and the National Research Foundation of Korea (NRF) grant funded by the Ministry of Science, ICT & Future Planning (MSIP) (NO. NRF-2015R1A5A1037627).

Reference

1. D. T. J. Hurlle, *Handbook of Crystal Growth*, 1993.
2. P. Hartman, *Crystal Growth: An Introduction*. Amsterdam: North Holland, 1973.
3. J. A. Venables, G. D. T. Spiller, and M. Hanbucken, "Nucleation and growth of thin films," *Reports on Progress in Physics*, vol. 47, pp. 399-459, 1984.
4. N. M. Hwang and D. Y. Yoon, "Thermodynamic approach to the paradox of diamond formation with simultaneous graphite etching in the low pressure synthesis of diamond," *Journal of Crystal Growth*, vol. 160, pp. 98-103, 1996.
5. N. M. Hwang, J. H. Hahn, and D. Y. Yoon, "Chemical potential of carbon in the low pressure synthesis of diamond," *Journal of Crystal Growth*, vol. 160, pp. 87-97, 1996.
6. N. M. Hwang, J. H. Hahn, and D. Y. Yoon, "Charged cluster model in the low pressure synthesis of diamond," *Journal of Crystal Growth*, vol. 162, pp. 55-68, 1996.
7. N. M. Hwang, "Non-Classical Crystallization of Thin Films and Nanostructures in CVD and PVD Processes", vol. 60: *Springer*, 2016.
8. A. Badzian, Hwang, N. M. , "Diamond: Low-Pressure Synthesis.," *Reference Module in Materials Science and Materials Engineering*, 2016.
9. B. W. Clare, G. Talukder, P. J. Jennings, J. C. L. Cornish, and G. T. Hefter, "Effect of charge on bond strength in hydrogenated amorphous silicon," *Journal of Computational Chemistry*, vol. 15, pp. 644-652, 1994.
10. N. M. Hwang, I. D. Jeon, and D. Y. Kim, *Ceramic Interfaces 2*. London: The Institute of Materials, 2001.
11. K. H. Homann and H. Wolf, "Charged soot in low-pressure acetylene/oxygen flames," *Symposium (International) on Combustion*, vol. 21, pp. 1013-1021, 1988.
12. N.M. Hwang and D. Y. Kim, "Charged clusters in thin film growth," *International Materials Reviews*, vol. 49, pp. 171-190, 2004.
13. J.-W. Park, K.-S. Kim, and N.-M. Hwang, "Gas phase generation of diamond nanoparticles in the hot filament chemical vapor deposition reactor," *Carbon*, vol. 106, pp. 289-294, 2016.
14. P. K. Chu and L. Li, "Characterization of amorphous and nanocrystalline carbon films," *Materials Chemistry and Physics*, vol. 96, pp. 253-277, 2006.
15. S. Praver and R. J. Nemanich, "Raman spectroscopy of diamond and doped diamond," *Philosophical Transactions of the Royal Society of London A: Mathematical, Physical and Engineering Sciences*, vol. 362, pp. 2537-2565, 2004.
16. S. Osswald and Y. Gogotsi, "In Situ Raman Spectroscopy of Oxidation of Carbon Nanomaterials," in *Raman Spectroscopy for Nanomaterials Characterization*, ed: Springer, pp. 291-351, 2012.
17. S. Osswald, G. Yushin, V. Mochalin, S. O. Kucheyev, and Y. Gogotsi, "Control of sp²/sp³ carbon ratio and surface chemistry of nanodiamond powders by selective oxidation in air," *Journal of the American Chemical Society*, vol. 128, pp. 11635-11642, 2006.
18. J. Cebik, J. K. McDonough, F. Peerally, R. Medrano, I. Neitzel, Y. Gogotsi, *et al.*, "Raman spectroscopy study of the nanodiamond-to-carbon onion transformation Dedicated to Professor Maurizio Prato on the occasion of his 60th birthday," *Nanotechnology*, vol. 24, p. 205703, 2013.
19. A. Sawabe and T. Inuzuka, "Growth of diamond thin films by electron assisted chemical vapor deposition.," *Applied Physics Letters*, 46 (2):146-147, 1985.
20. A. Sawabe and T. Inuzuka, "Growth of diamond thin films by electron-assisted chemical vapour deposition and their characterization," *Thin Solid Films*, vol. 137, pp. 89-99, 1986.
21. N. M. Hwang and D. K. Lee, "Charged nanoparticles in thin film and nanostructure growth by chemical vapour deposition," *Journal of Physics D: Applied Physics*, vol. 43, 483001, 2010.
22. I. D. Jeon, C. J. Park, D. Y. Kim, and N. M. Hwang, "Experimental confirmation of charged carbon clusters in the hot filament diamond reactor," *Journal of Crystal Growth*, vol. 213, pp. 79-82, 2000.
23. I. D. Jeon, C. J. Park, D.-Y. Kim, and N. M. Hwang, "Effect of methane concentration on size of charged clusters in the hot filament diamond CVD process," *Journal of Crystal Growth*, vol. 223, pp. 6-14, 2001.